

# Recombinase-Aided Amplification Combined with Lateral Flow (LF-RAA) Assay for Rapid AAV Genome Detection

Kun Wang, Ruolan Huang, Liyun Zhang, Dan Liu,\* and Yong Diao\*

Cite This: *ACS Omega* 2022, 7, 47832–47839

Read Online

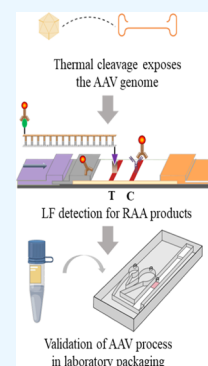
ACCESS |

Metrics &amp; More

Article Recommendations

Supporting Information

**ABSTRACT:** Adeno-associated virus (AAV) is a versatile gene vector that is widely used in mammalian research. In basic studies and large-scale AAV production, genetic testing is ubiquitous and routine polymerase chain reaction (PCR)-based tests limit the efficiency due to the labor-intensive and time-consuming requirements of thermal cycling. This study introduces an assay based on recombinase-aided amplification combined with lateral flow (LF-RAA), which can quickly and accurately detect the AAV genome, thus improving the efficiency of AAV research and production. This application is the first use of an RAA approach to AAV genome detection. In this point-of-care testing (POCT) detection platform, the RAA reaction and LF readout are integrated into a user-friendly microfluidic chip that can be applied without advanced technical training. The LF-RAA chip provides high sensitivity, with a limit of detection of 10 copies/ $\mu\text{L}$ , and generates results quickly, and it only needs to be incubated for 10 min at a constant temperature, that is, 39 °C. Results are visualized on the LF Dipstick, and detection results are reliable, validated with 100% accuracy in 47 laboratory-produced recombination adeno-associated virus (rAAV) samples carrying target genes from several different viruses. The LF-RAA assay is applicable in AAV research and production processes requiring genome identification.



## INTRODUCTION

Adeno-associated virus (AAV) is a small, non-enveloped virus consisting of a 25 nm icosahedral capsid protein and a single-stranded ~4.7 kb linear DNA genome.<sup>1</sup> AAV offers several advantages as an expression vector in laboratory research: (1) it is expressed in long-term, stable, and high levels and (2) the virus has low genotoxicity and therefore relatively high safety.<sup>2–4</sup> Since the discovery of AAV in a laboratory preparation of adenovirus (ADV) in the mid 1960s, a vast multitude of studies involving AAV have been carried out, due in part to its importance as a vector in the field of gene therapy.<sup>5,6</sup> To date, research interest in AAV has continually increased, and many AAV therapeutic agents have been approved for clinical treatment of numerous diseases, including coagulation disorders, hereditary blindness, and neurodegenerative diseases among others.<sup>7,8</sup> In addition, a variety of AAV gene therapy products are still in clinical trials, all of which support the ongoing intense focus on AAV-related research topics, such as the potential relationship between the AAV capsid protein and therapeutic effects,<sup>9</sup> the relationship between the AAV genome and its in vivo transduction efficiency,<sup>10,11</sup> the association between various regulatory elements in the AAV genome and recombinant AAV (rAAV) yield,<sup>12,13</sup> mechanisms of the AAV genome corresponding with specific functions,<sup>14,15</sup> etc.

The vast majority of studies on AAV involve the detection of rAAV genomes for qualitative or quantitative analysis.<sup>16,17</sup> As early as 1997, Allen and colleagues described the identification and elimination of replication competent AAV (rcAAV) that appeared during rAAV production.<sup>18</sup> In that work, PCR

reaction of the D-region-Rep or D-region-Cap genes in rcAAV followed by Southern blot analysis was used to confirm the presence of rcAAV. This highly sensitive analytical method provides reliable detection results and is simple to perform, and consequently, is still widely used. However, each experiment is time-consuming, requiring 2 h or longer for PCR and electrophoresis, thus limiting research progress to some extent.

In addition, during rAAV packaging, other nearby deoxyribonucleic acid (DNA) can also be loaded into the capsid, including host cell DNA and plasmid backbone DNA.<sup>19</sup> These rAAV carriers of non-target genes can be harmful to therapies by reducing the purity of therapeutic rAAVs and potentially triggering an immune response. To address this issue, Schnodt and co-workers proposed a microloop (MC) construct for the production of single-stranded (ss) and self-complementary (sc) AAV vectors to replace AAV vectors and auxiliary plasmids and to improve the purity of AAV preparations.<sup>20</sup> Quantitative real-time PCR (qPCR) is mainly used in that research to verify the effects on AAV packaging. As the gold standard for nucleic acid detection, qPCR is widely used in gene expression research, transgenic research, titer

Received: September 1, 2022

Accepted: November 18, 2022

Published: December 15, 2022



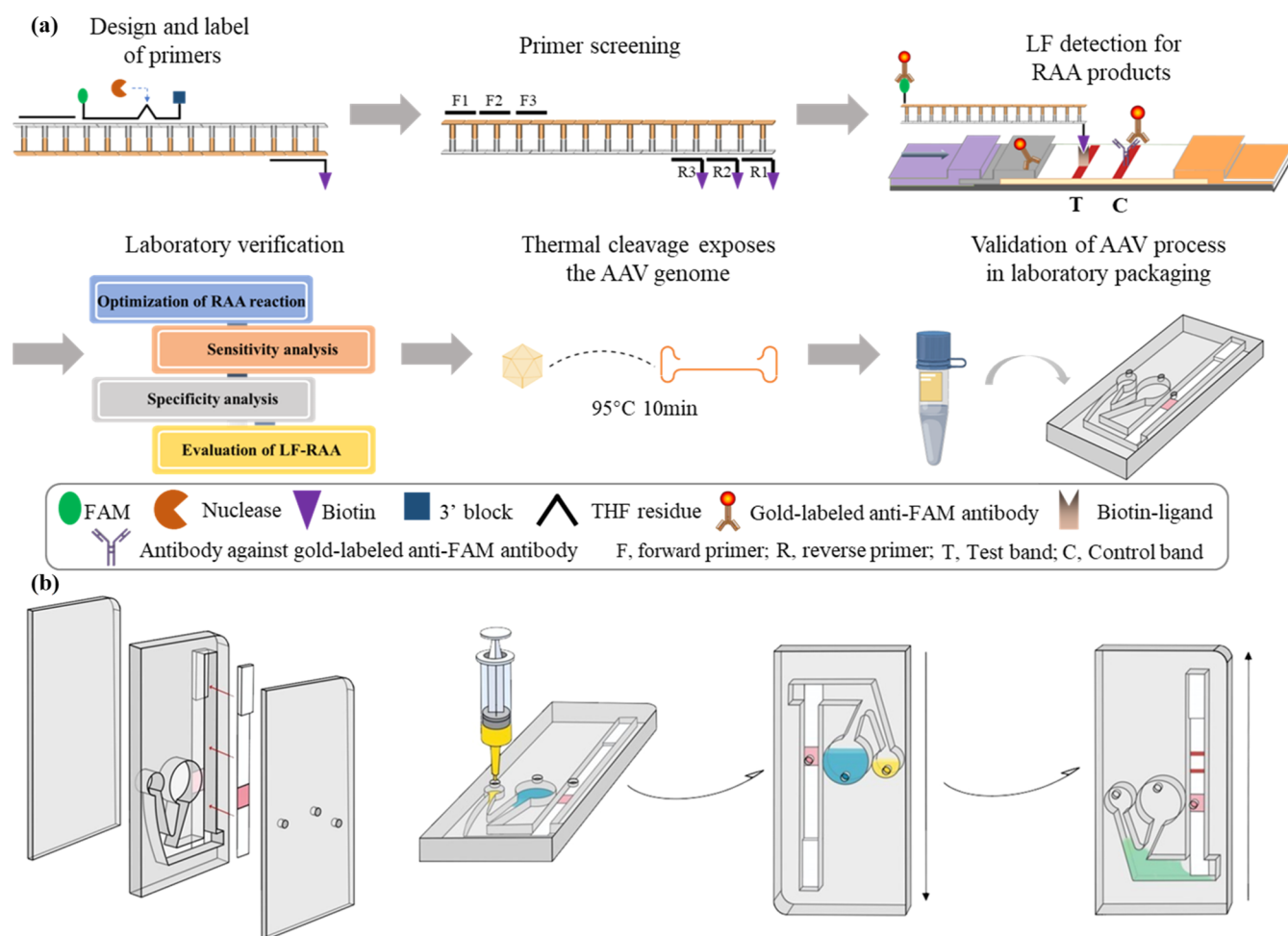


**Figure 1.** Schematic diagram of LF-RAA detection of AAV genome. (a) Flow of AAV-LF detection. The research includes the design of primers and probes, the screening of primer pairs with excellent performance, and the comprehensive evaluation of the performance of the LF-RAA assay. Finally, the entire LF-RAA process was integrated into a microfluidic chip for POCT of clinical samples (AAV), which had their genomes exposed by thermal lysis prior to detection. The experimental protocol is designed to ensure reliable validation results, while greatly reducing the cost of the research process. (b) Microfluidic chip structure diagram and the flow of integrated detection.

detection, pathogen detection, and many other fields due to its advantages of high accuracy and good reproducibility. However, qPCR needs to be carried out using a specialized instrument that requires technical training, and so, studies involving qPCR assays are typically conducted in fully equipped laboratories.

## EXPERIMENTAL SECTION

The development of a simple, rapid, and reliable method for qualitative detection of the AAV genome can improve the genetic screening process in AAV research and production, thus improving efficiency and reducing AAV production time and costs. In this study, we describe a LF-RAA assay for rapid qualitative detection of AAV genomes. Similar to the principle of recombinase polymerase amplification (RPA), RAA occurs at a constant temperature amplification reaction, as first reported by Armes et al. in 2006.<sup>21</sup> Although this technology was introduced relatively late, it developed rapidly and was soon widely applied in nucleic acid detection. The RAA reaction can be completed in 10 min at 39 °C.<sup>22</sup> Using a specially engineered Nfo endonuclease probe with a universal lateral-flow (LF) strip for capture of biotin and FAM-labeled analytes, the results can be quickly visualized without

additional detection equipment. The control band (C) in the LF readout validates the correct function of the LF capture, while the red test band (T) indicates a positive test result, and no band is a negative result. To exploit these advantages of LF-RAA, we constructed a chip for rapid detection of the AAV genome. To further simplify the AAV genome detection process and reduce the likelihood of cross-contamination, we integrated the RAA reaction and LF readout components into an integrated, closed, microfluidic chip platform. We then experimentally validated the performance of this integrated platform and performed a qualitative analysis of 47 in vitro-packaged AAVs. The results showed that this chip-based platform can accurately detect the AAV genome within 10 min. Thus, through its operational simplicity, this functionally integrated LF-RAA assay can effectively improve the efficiency of AAV research and production, without detriment to its accuracy or sensitivity, and can be easily adopted by any laboratory engaged in AAV research.

## RESULTS AND DISCUSSION

**LF-RAA DNA Amplification Technology for Rapid AAV Genome Detection.** Herein, we developed a rapid, sensitive, and accurate integrated platform for AAV genome

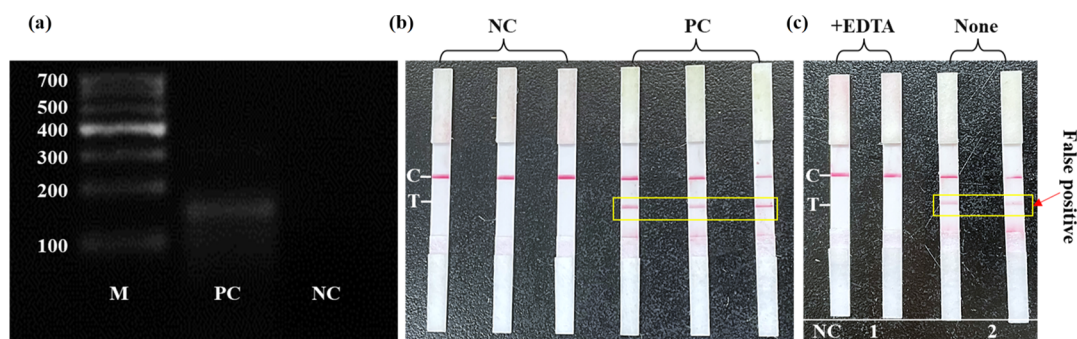


**Figure 2.** Screening of RAA primers and optimization of the LF-RAA reaction system. (a) Agarose gel electrophoresis to verify the effect of F2-R3 primer pair for RAA reaction. (b) Validation of LF-AAV detection by F2-R3 primer pair. (c) Optimized LF-RAA detection method.

detection. **Figure 1a** shows the underlying principles and basic protocol steps. First, the AAV capsid protein is disrupted by thermal cleavage to expose the genome. Then, the RAA primers and probe for the target gene of AAV [or enhanced green fluorescent protein (EGFP) gene] are amplified at 39 °C at a constant temperature. Finally, the amplification products are captured on the LF readout strip. More specifically, the amplification products carry FAM and biotin labels; FAM is used to bind anti-FAM antibody-modified nanogold particles and biotin is used to bind biotin-ligand immobilized in the test band. The amplification product bound to nanogold aggregates in the test band by chromatography to produce a visual band. In the absence of the target gene, no amplification product accumulates and the nanogold only forms a visible band through binding species-specific antibodies in the control band region of the LF readout. The user then determines a positive or negative result by simply looking at the band. During development and validation, several sets of RAA primers were screened. To improve RAA reaction robustness against aerosol contamination and to simplify the protocols, we integrated the reaction and readout components of the AAV-LF assay into a closed, microfluidic chip and tested the platform accuracy and effectiveness in detecting several constructs packaged in the AAV vector. **Figure 1b** shows the structure of the integrated chip, with the cover and base plates glued together in a sandwich format to seal the RAA and LF chambers, as well as the workflow for operating the chip. The RAA reaction solution (yellow) and the running buffer (blue) are transferred to the corresponding chambers through the inlet hole, and a transparent adhesive is applied to prevent the liquid from leaking. After 10 min, the chip is stood on its end and gently shaken to mix the RAA reaction solution with running buffer. The assay results are finally displayed in the LF readout.

**Optimization of the RAA Reaction System.** Before testing the AAV genome, we screened RAA primer pairs targeting the EGFP gene. Three candidate forward primers (F1, F2, and F3) and three reverse primers (R1, R2, and R3) were selected near the position of the Nfo probe. The primers were initially evaluated using Primer Premier 5 software to avoid nucleotide chains that were likely to form hairpin structures or dimers. As shown in **Figure 2a**, RAA amplification products were verified by agarose gel electrophoresis, and the F2-R3 primer pair showed the strongest target amplification. The primer pair was combined with the Nfo probe for LF-AAV assays, and the experimental groups included negative and positive controls, with three parallel replicates for each sample, as shown in **Figure 2b**. Since  $Mg^{2+}$  initiates the RAA reaction, the reaction was terminated by addition of 2  $\mu$ L ethylene

diamine tetraacetic acid (EDTA) through chelation of  $Mg^{2+}$ , after 10 min of amplification. Using EDTA to limit reaction time, the number of false positive results markedly decreased (**Figure 2c**). In particular, LF readouts after 15 min of RAA reaction, in the absence of template, showed obvious positive results (**Figure 2c**, right), while these artifactual bands were eliminated in tubes where EDTA was used to stop the reaction after 10 min (**Figure 2c**, left). These results indicated that the accuracy gene detection with the LF-RAA assay was substantially improved through the addition of EDTA as a reaction terminator.

#### CONSTRUCTION OF THE LF-RAA DETECTION SYSTEM ON A PLASMID EXPRESSION VECTOR

To ensure that the POCT platform for detecting the AAV genome was sufficiently fast, accurate, sensitive, and convenient for deployment in clinical settings, the LF-RAA assay performance was validated through a series of AAV detection experiments. Since the AAV genome is enveloped by the capsid protein, which prevents its direct detection, bare plasmids were used to first investigate the specificity, sensitivity, and accuracy of the assay, as is standard practice for validating conventional nucleic acid tests.<sup>23</sup> For this purpose, we generated a plasmid expression construct containing inverted terminal repeats (ITRs), wood chuck hepatitis virus post transcriptional regulation element (WPRE) as well as a 714 sequence encoding EGFP driven by the SV40 promoter. After verifying that the F2-R3/LF primer pair/probe set could amplify the EGFP gene (**Figure 3a**), we next tested the assay specificity using two plasmids lacking the EGFP gene (i.e., pAAV-H22 and pAAV-Fd6) as well as DNA fragments of other viral genes from H7N9-NA, SARS-CoV-2 ORF1ab, and SARS-CoV-2 PABPC4. All detection assays were conducted with three replicates, which showed that only samples containing the EGFP target gene produced a positive test band in LF readouts, while samples with other viral genes did not, indicating that the LF-RAA had good specificity (**Figure 3b**). The AAV genome load is small and the three plasmids already contain the entire rAAV genome as well as the wild-type AAV genome. Details of the three plasmids are shown in **Supporting Information 7**. That is, specificity validation on the plasmids is an economical and efficient way to reduce unnecessary overhead in the study, and the non-target genes used for the abovementioned specificity validation are not additionally constructed for rAAV.

In light of these results validating the specificity of LF-RAA assay, assay sensitivity was then examined using a pAAV-EGFP template concentration gradient of 1–10<sup>4</sup> copies/ $\mu$ L with



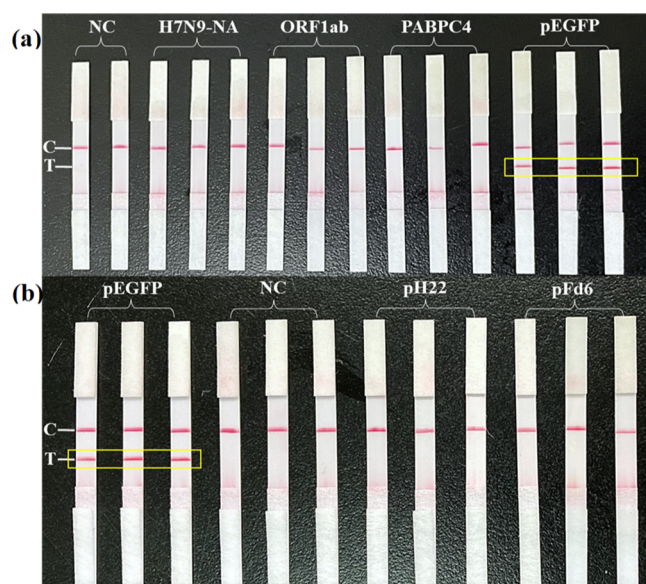


**Figure 3.** LF-RAA specificity test for EGFP gene. (a) Specificity of three viral nucleic acid sites (H7N9 NA, SARS-CoV-2 ORF1ab, and SARS-CoV-2 PABPC4) was detected by LF. (b) Specificity of three plasmids (pEGFP, pH22, and pFd6) was detected by LF.

diethylpyrocarbonate (DEPC) H<sub>2</sub>O as a negative control. The pAAV-EGFP quantitative analysis is performed, as shown in Supporting Information 6. Close examination of the LF readouts for each assay showed that EGFP copy numbers as low as 10<sup>1</sup> copies/ $\mu$ L produced a positive test band (Figure 4a). In order to present the detection results more visually, the test bands were analyzed in grayscale (Supporting Information 8). Band intensity quantification by gray value analysis with Image J software further supported 10 copies/ $\mu$ L as the limit of detection (LOD) (Figure 4b). By contrast, qPCR assays using the same template concentrations showed an LOD of 10<sup>3</sup> copies/ $\mu$ L (Figure 4c). Taken together, these results indicated that the LF-RAA assay provides high specificity and sensitivity, especially in comparison with qPCR, the current gold standard for nucleic acid detection.

Next, the accuracy of the LF-RAA assay was examined using nine randomized samples with or without the EGFP target gene (Supporting Information 2). Three of the nine samples contained 10<sup>2</sup>, 10<sup>3</sup>, or 10<sup>7</sup> copies/ $\mu$ L of the target gene, while the remaining samples had either DEPC H<sub>2</sub>O in place of template or non-target viral genes used in the abovementioned specificity assays. All samples were randomized and technicians were blinded to sample content; qPCR was used to verify the results. The detection assays were performed in triplicate and showed three positive results (Figure 5), which was consistent with the number of positive samples. Notably, only two positive samples were detected by qPCR, indicating the occurrence of a false negative due to the target concentration of 10<sup>2</sup> copies/ $\mu$ L in one sample, which was below the LOD for qPCR using this primer/probe set. In addition, the results of the blind tests correctly identified the positive samples.

**AAV Lysis to Expose Nucleic Acids.** Based on the abovementioned results showing that the LF-RAA assay system could detect plasmid-borne target DNA, the system was then modified for detection of the AAV genome.<sup>24,25</sup> For this purpose, it was first necessary to establish AAV sample processing protocols for releasing viral DNA from the capsid. Mechanical or chemical lysis methods are commonly used in

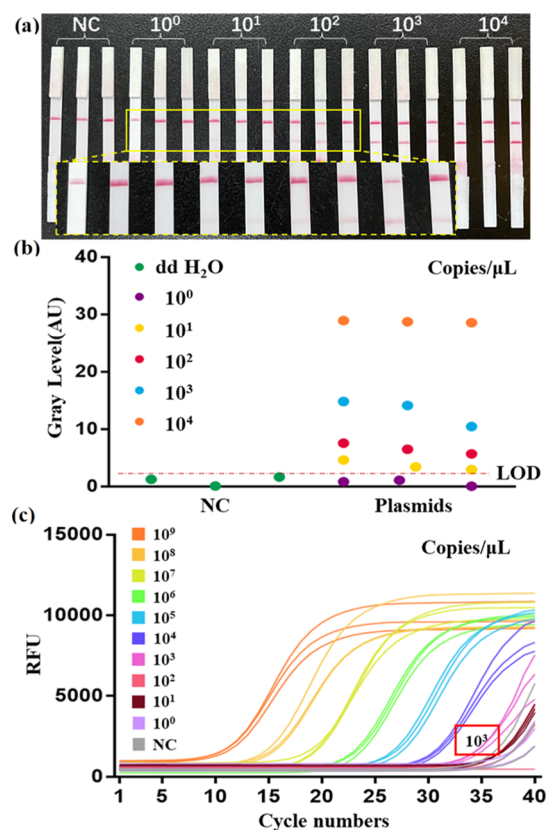


**Figure 4.** LF-RAA assay system sensitivity test (a). Target plasmids with concentrations of 1–10<sup>4</sup> copies/ $\mu$ L were detected by LF. (b) Gray value of the positive signal in the LF in A and red line indicates lowest of detection (LOD). (c) Gold standard qPCR for genetic testing was used to detect target plasmids at concentrations of 1–10<sup>9</sup> copies/ $\mu$ L.

virus detection,<sup>28,30</sup> including repeated freeze–thaw cycles, high-temperature lysis, lysis in concentrated salt solutions, proteolysis, etc. In laboratory research, lysis with proteinase K is the most widely used approach, although the process is relatively time-consuming (i.e., >1 h) and not well suited for point of care testing. While lysis in high salt solution is simpler, purification is then necessary after lysis to prevent the salt from interfering with the RAA reaction. In contrast, high-temperature lysis can be conducted in less time, using simple protocols and equipment conducive to point of care application and without introducing agents that could disrupt the RAA reaction.

Heat lysis at 95 °C was then compared with proteinase K lysis using freshly prepared AAV9 solutions at a range of virus particle concentrations. The relative extraction efficiency was then quantified for both lysis methods by qPCR. The results showed that both methods yielded comparable levels of detectable virus DNA (Figure 6a). However, at low concentrations, the difference between high-temperature and proteinase K lysis was more obvious due to the presence of residual proteinase K in the AAV9 solution. Additionally, the high-temperature lysis required considerably less time for sample processing than the enzymatic lysis method, although the results were similarly effective. Thus, the high-temperature lysis method was used to process AAV samples in subsequent experiments.

**POCT Workflow for AAV.** Since the ultimate purpose of the LF-RAA assay system was for point-of-care detection



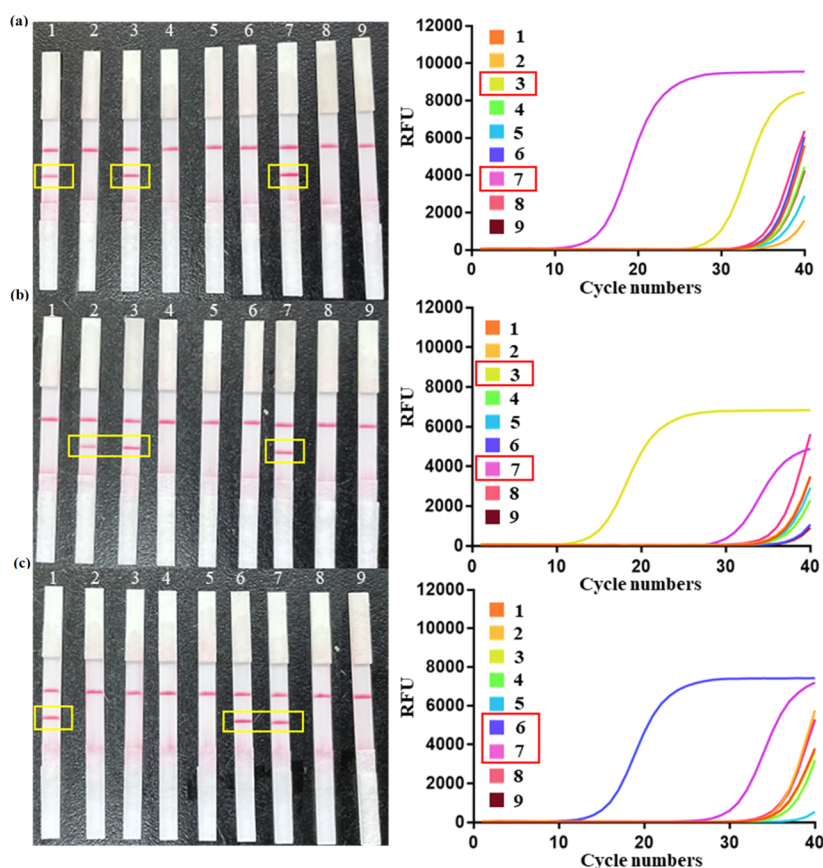


**Figure 5.** LF-RAA assay system accuracy test. Nine samples were tested repeatedly for three times. The samples were disordered before each test, and LF-RAA and qPCR were set for each test. LF-RAA assay is on the left and qPCR detection is on the right. (a) First random detection. (b) Second random detection. (c) Gold standard qPCR for genetic testing was used to detect target plasmids at concentrations of  $1\text{--}10^9$  copies/ $\mu\text{L}$ .

during rAAV production and other processes requiring rAAV screening, we then loaded the LF-RAA assay system into the chip and constructed the integrated POCT platform, which simplified the assay process while decreasing the possibility of aerosol contamination. The microfluidic chip fabrication process integrates the RAA reaction chamber and LF readout in a single chip (Supporting Information 5).

In addition, the MI-LF-RAA POCT platform is simple to operate (Figure 1b): the AAV samples were lysed in heat block or water bath at  $95\text{ }^\circ\text{C}$  for 10 min, during which  $200\text{ }\mu\text{L}$  of EDTA-Running Buffer was added to the buffer chamber through inlet hole b in the chip (Figure 6b). Then,  $42.5\text{ }\mu\text{L}$  of RAA master mix (containing RAA enzyme, buffer A, RAA primer, and probe) was added to inlet hole c in the reaction chamber. After the AAV samples were processed,  $5\text{ }\mu\text{L}$  of the sample was added through inlet hole c. Finally,  $2.5\text{ }\mu\text{L}$  of buffer B was added to initiate the RAA reaction. To avoid leakage of the reaction mixture from the inlet holes, the holes were sealed with tape. After incubation at  $39\text{ }^\circ\text{C}$  for 10 min, the chip was then placed in a vertical position and gently shaken to mix the liquids from the reaction and buffer chambers in the channel at the bottom of the chip. The assay results appeared on the LF chamber within 5 min after wetting the LF sample pad. In addition to its accuracy and reliability, the abovementioned MI-LF-RAA POCT workflow requires less than 20 min from the start of the RAA reaction to reading the test results. The simplicity of the operation makes it possible for non-specialist researchers to master it quickly with limited training. This POCT platform was also used to test three serotypes of AAV

(AAV2, AAV9, and AAV-PHP.eB) carrying the EGFP gene at a concentration of  $10\text{ copies}/\mu\text{L}$ , all of which produced positive results (Figure 6b).

**Validation of the AAV Process in Laboratory Packaging.** To validate the performance of the device, we performed POCT on 47 rAAVs packed in different batches,<sup>26</sup> of which carried the EGFP gene and 21 that did not. In randomized, blinded assays, all positive samples were detected as positive, while all negative samples and controls produced negative results (Figure 6c; Supporting Information 5). These results strongly supported the further use of the assay in rAAV research and production. Moreover, this method could potentially improve the efficiency of quality control and contamination monitoring in rAAV production. It should be noted that the deployment of this POCT platform in commercial rAAV production requires the prior cleavage of residual nucleic acids in the cytoplasm with DNase I or other enzymes to avoid possible downstream impacts on the assay results.

**Challenges and Future Perspectives.** Currently, the assay is only suitable for rAAV production applications that need rapid qualitative or semiquantitative rAAV detection to make relevant adjustments to rAAV production conditions. The assay can be similarly useful in research examining AAV mechanisms that require qualitative or semiquantitative screens.<sup>27,28</sup> However, in large-scale production of rAAV, quantitative assays are necessary for quality control in order to ensure high concentrations and purity of rAAV. This may limit the extent to which the assay can replace qPCR assays.<sup>6,29,30</sup> In

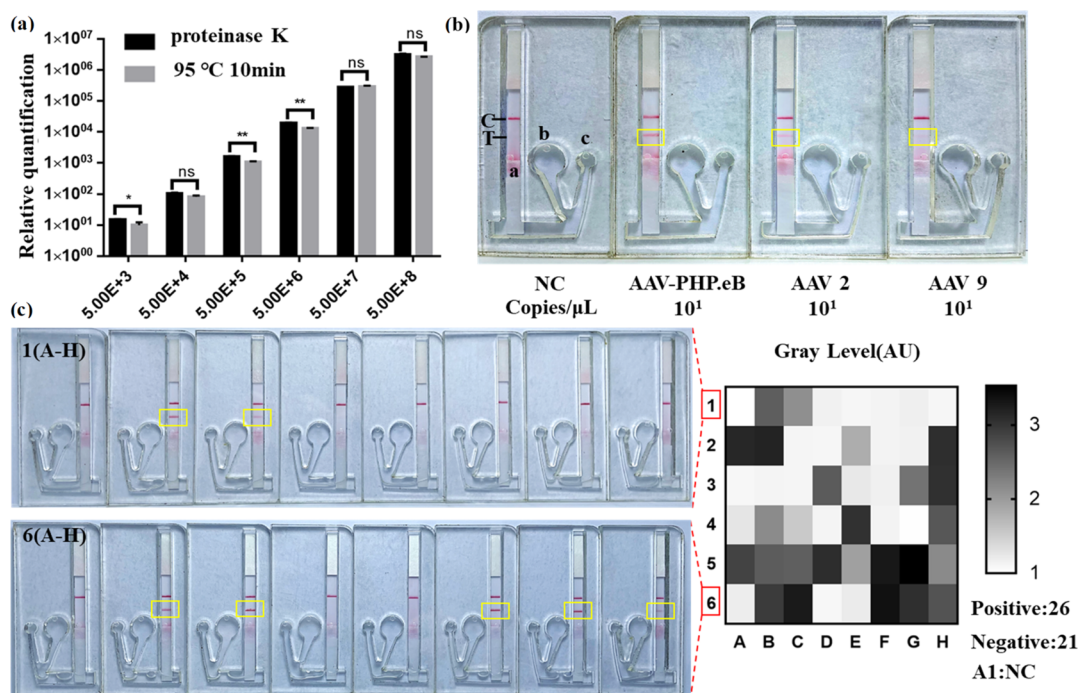


**Figure 6.** (a) Comparison of the effects of thermal lysis and protease k lysis on AAV. (b) MI-LF-RAA platform detects three serotypes of AAV carrying target genes. Inlet hole a, test strip channel; inlet hole b, running buffer chamber; and inlet hole c, RAA reaction chamber. (c) Results of testing packaged rAAV samples with the MI-LF-RAA device. Of the 47 samples tested, 26 were positive and 21 were negative, which was consistent with the number of rAAVs carrying the EGFP or Luc genes. On the left are representative results of the MI-LF-RAA device assay corresponding to rows 1 and 6 of the grayscale band intensity analysis (right) performed with Image J. The gray level (AU) in the heat map is the ratio of each clinical test result to the negative control; the more distinct the visualized bands (Test Band), the higher the relative gray level. A1 is the negative control.

addition, many AAV research projects require multi-locus testing of the rAAV genome, such as studying the effects of various components of the AAV genome on rAAV yield. Incomplete rAAV is most commonly found as empty capsid proteins or a capsid protein wrapped around an incomplete DNA strand.<sup>31,32</sup> Incomplete DNA strands generally result in a variety of transcribed isoforms due to differing lengths of the lost DNA segments, making it impossible to determine the integrity of rAAV through detection of a single locus, since the truncated DNA strand may contain the detection site. To reliably determine rAAV genome integrity, at least three loci must be checked, two of which are located near the two ITR sequences, while the other site is within the target gene.

Thus, the POCT platform can be improved by enhancing the accuracy of its quantification and by incorporating multi-locus detection. At present, accurate quantification by RAA or other thermostatic amplification techniques remains out of reach, probably because RAA uses increasingly complex enzymes compared to those used in PCR. Although the complexity of the RAA reaction system is related to power and robustness of its detection, the complexity of the enzymatic mixture also directly affects the stability of RAA. Therefore, an accurate, quantitative RAA system must be further optimized and its stability enhanced. Some progress has already begun in the optimization of an RAA reaction system, supporting the feasibility of further optimization and reaction stabilization.

By contrast, it may be quite feasible to incorporate multi-locus detection by the chip. In this case, the only obvious obstacle is related to RAA primer/probe design. Since RAA primers and probes are relatively long ( $30 \pm 2$  nt for primers and 46–52 nt for probes), they may form dimers, hairpins, or

other secondary structures at room temperature, impeding the RAA template amplification. However, multi-locus detection can be achieved through rational identification of detection sites and design and screening of RAA primers and probes. Alternatively, multi-locus detection in point-of-care testing could be conducted by developing a multi-channel microfluidic chip.

Advances in these two aspects will greatly enhance the application value of the integrated POCT platform in rAAV genome detection. In particular, accurate quantification with an RAA system could revolutionize POCT applications of RAA or similar thermostatic amplification technologies (such as RPA, ERA, etc).

## CONCLUSIONS

LF-RAA assay has the advantages of easy operation, high sensitivity, and high specificity with no dependence on large equipment. The POCT platform incorporates advantages of both the LF and RAA technologies by integrating the reaction and readout components on a small chip. The assay works by simply initiating the reaction at 39 °C for 10 min, then placing the chip upright, and shaking it gently. The assay results are usually available within 5 min. Through our optimization of the RAA reaction, long reactions do not lead to false positive results. The sensitivity of the LF-RAA assay can reach 10 copies/ $\mu$ L, and it also performs well in high specificity detection scenarios, whether for the other two plasmids (pAAV-H22, pAAV-Fd6) in the triple plasmid transfection method of AAV packaging, or for partial nucleic acids of other viruses (Flu, COVID-19: ab1, ab4), no amplification reaction occurs. Accuracy was verified by qPCR, which were consistent

with LF-RAA assay results, although LF-RAA was more accurate at lower sample concentrations. In an experiment testing 47 different serotypes of rAAV carrying different target genes packaged in the laboratory, including 26 groups of positive samples carrying target genes, 21 groups of negative samples carrying non-target genes, and one group of negative controls, the assay showed 100% accuracy.

We thus verified the performance of the LF-RAA assay system through multiple experiments, which together demonstrated the platform's capability for genetic testing in rAAV research, production, and other processes. In particular, this platform is suitable for applications requiring the detection of DNA impurities in rAAV and studies of the function of individual components in the AAV genome that need only qualitative testing of the rAAV genome, but for a large number of replicates.

In conclusion, we provide the first demonstration of the feasibility of the LF-RAA assay for rAAV genomic testing, and our results support its application and potential for further development. Future work will examine possible adaptations for other testing applications in nucleic acid production and research.

## ■ ASSOCIATED CONTENT

### SI Supporting Information

The Supporting Information is available free of charge at <https://pubs.acs.org/doi/10.1021/acsomega.2c05660>.

Materials and reagents used for experiments and experimental data, including oligonucleotide design, microfluidic chip fabrication method, and initial data of laboratory-packaged rAAV genomic assay results (PDF)

## ■ AUTHOR INFORMATION

### Corresponding Authors

Dan Liu – Department of Biological Engineering, School of Medicine, Huaqiao University, Quanzhou 362021, China; [orcid.org/0000-0001-8751-3455](https://orcid.org/0000-0001-8751-3455); Email: [liudan@hqu.edu.cn](mailto:liudan@hqu.edu.cn)

Yong Diao – Department of Biological Engineering, School of Medicine, Huaqiao University, Quanzhou 362021, China; Email: [diaoyong@hqu.edu.cn](mailto:diaoyong@hqu.edu.cn)

### Authors

Kun Wang – Department of Biological Engineering, School of Medicine, Huaqiao University, Quanzhou 362021, China

Ruolan Huang – Department of Biological Engineering, School of Medicine, Huaqiao University, Quanzhou 362021, China

Liyun Zhang – Department of Biological Engineering, School of Medicine, Huaqiao University, Quanzhou 362021, China

Complete contact information is available at:

<https://pubs.acs.org/doi/10.1021/acsomega.2c05660>

### Notes

The authors declare no competing financial interest.

## ■ ACKNOWLEDGMENTS

We thank the the Natural Science Foundation of Fujian Province, China (2021J01310), Fujian Province Young and Middle-aged Teachers' Educational Research Projects (JAT210888), Science and Technology Project of Quanzhou (2020SY002), Fundamental Research Funds for the Central

Universities (ZQN-818), and State Key Laboratory of Chemo/Biosensing and Chemometrics (2019006). Some of the images in this paper were drawn on the Figdraw platform, thanks to Figdraw's support.

## ■ REFERENCES

- (1) Samulski, R. J.; Muzyczka, N. AAV-Mediated Gene Therapy for Research and Therapeutic Purposes. *Annu. Rev. Virol.* **2014**, *1*, 427–451.
- (2) Hudry, E.; Vandenberghe, L. H. Therapeutic AAV Gene Transfer to the Nervous System: A Clinical Reality. *Neuron* **2019**, *101*, 839–862.
- (3) Carter, B. J. Adeno-Associated Virus and the Development of Adeno-Associated Virus Vectors: A Historical Perspective. *Mol. Ther.* **2004**, *10*, 981–989.
- (4) Wang, D.; Tai, P. W. L.; Gao, G. Adeno-Associated Virus Vector as a Platform for Gene Therapy Delivery. *Nat. Rev. Drug Discovery* **2019**, *18*, 358–378.
- (5) Sonntag, F.; Schmidt, K.; Kleinschmidt, J. A. A Viral Assembly Factor Promotes AAV2 Capsid Formation in the Nucleolus. *Proc. Natl. Acad. Sci.* **2010**, *107*, 10220–10225.
- (6) Li, C.; Samulski, R. J. Engineering Adeno-Associated Virus Vectors for Gene Therapy. *Nat. Rev. Genet.* **2020**, *21*, 255–272.
- (7) Colella, P.; Ronzitti, G.; Mingozzi, F. Emerging Issues in AAV-Mediated In Vivo Gene Therapy. *Mol. Ther. - Methods Clin. Dev.* **2018**, *8*, 87–104.
- (8) Mendell, J. R.; Al-Zaidy, S. A.; Rodino-Klapac, L. R.; Goodspeed, K.; Gray, S. J.; Kay, C. N.; Boye, S. L.; Boye, S. E.; George, L. A.; Salabarria, S.; Corti, M.; Byrne, B. J.; Tremblay, J. P. Current Clinical Applications of In Vivo Gene Therapy with AAVs. *Mol. Ther.* **2021**, *29*, 464–488.
- (9) Büning, H.; Srivastava, A. Capsid Modifications for Targeting and Improving the Efficacy of AAV Vectors. *Mol. Ther. - Methods Clin. Dev.* **2019**, *12*, 248–265.
- (10) Rabinowitz, J. E.; Rolling, F.; Li, C.; Conrath, H.; Xiao, W.; Xiao, X.; Samulski, R. J. Cross-Packaging of a Single Adeno-Associated Virus (AAV) Type 2 Vector Genome into Multiple AAV Serotypes Enables Transduction with Broad Specificity. *J. Virol.* **2002**, *76*, 791–801.
- (11) McCarty, D.; Monahan, P.; Samulski, R. Self-Complementary Recombinant Adeno-Associated Virus (ScAAV) Vectors Promote Efficient Transduction Independently of DNA Synthesis. *Gene Ther.* **2001**, *8*, 1248–1254.
- (12) Wu, Z.; Yang, H.; Colosi, P. Effect of Genome Size on AAV Vector Packaging. *Mol. Ther.* **2010**, *18*, 80–86.
- (13) McCarty, D. M.; Fu, H.; Monahan, P. E.; Toulson, C. E.; Naik, P.; Samulski, R. J. Adeno-Associated Virus Terminal Repeat (TR) Mutant Generates Self-Complementary Vectors to Overcome the Rate-Limiting Step to Transduction in Vivo. *Gene Ther.* **2003**, *10*, 2112–2118.
- (14) Girod, A.; Wobus, C. E.; Zádori, Z.; Ried, M.; Leike, K.; Tijssen, P.; Kleinschmidt, J. A.; Hallek, M. The VP1 Capsid Protein of Adeno-Associated Virus Type 2 Is Carrying a Phospholipase A2 Domain Required for Virus Infectivity. *J. Gen. Virol.* **2002**, *83*, 973–978.
- (15) Hirata, R. K.; Russell, D. W. Design and Packaging of Adeno-Associated Virus Gene Targeting Vectors. *J. Virol.* **2000**, *74*, 4612–4620.
- (16) Mietzsch, M.; Eddington, C.; Jose, A.; Hsi, J.; Chipman, P.; Henley, T.; Choudhry, M.; McKenna, R.; Agbandje-McKenna, M. Improved Genome Packaging Efficiency of Adeno-Associated Virus Vectors Using Rep Hybrids. *J. Virol.* **2021**, *95*, 007733–e821.
- (17) Hirsch, M. L.; Storici, F.; Li, C.; Choi, V. W.; Samulski, R. J. AAV Recombineering with Single Strand Oligonucleotides. *PLoS ONE* **2009**, *4*, No. e7705.
- (18) Allen, J. M.; Debelak, D. J.; Reynolds, T. C.; Miller, A. D. Identification and Elimination of Replication-Competent Adeno-Associated Virus (AAV) That Can Arise by Nonhomologous



Recombination during AAV Vector Production. *J. Virol.* **1997**, *71*, 6816–6822.

(19) Chadeuf, G.; Ciron, C.; Moullier, P.; Salvetti, A. Evidence for Encapsidation of Prokaryotic Sequences during Recombinant Adeno-Associated Virus Production and Their in Vivo Persistence after Vector Delivery. *Mol. Ther.* **2005**, *12*, 744–753.

(20) Schnödt, M.; Schmeer, M.; Kracher, B.; Krüsemann, C.; Espinosa, L. E.; Grünert, A.; Fuchsluger, T.; Rischmüller, A.; Schleaf, M.; Büning, H. DNA Minicircle Technology Improves Purity of Adeno-Associated Viral Vector Preparations. *Mol. Ther. - Nucleic Acids* **2016**, *5*, No. e355.

(21) Li, J.; Macdonald, J.; von Stetten, F. Review: A Comprehensive Summary of a Decade Development of the Recombinase Polymerase Amplification. *The Analyst* **2019**, *144*, 31–67.

(22) Lobato, I. M.; O'Sullivan, C. K. Recombinase Polymerase Amplification: Basics, Applications and Recent Advances. *TrAC Trends Anal. Chem.* **2018**, *98*, 19–35.

(23) Wang, X.; Kong, D.; Guo, M.; Wang, L.; Gu, C.; Dai, C.; Wang, Y.; Jiang, Q.; Ai, Z.; Zhang, C.; Qu, D.; Xie, Y.; Zhu, Z.; Liu, Y.; Wei, D. Rapid SARS-CoV-2 Nucleic Acid Testing and Pooled Assay by Tetrahedral DNA Nanostructure Transistor. *Nano Lett.* **2021**, *21*, 9450–9457.

(24) McNally, D. J.; Piras, B. A.; Willis, C. M.; Lockey, T. D.; Meagher, M. M. Development and Optimization of a Hydrophobic Interaction Chromatography-Based Method of AAV Harvest, Capture, and Recovery. *Mol. Ther. - Methods Clin. Dev.* **2020**, *19*, 275–284.

(25) Powers, A. D.; Piras, B. A.; Clark, R. K.; Lockey, T. D.; Meagher, M. M. Development and Optimization of AAV HFIX Particles by Transient Transfection in an ICELLis<sup>®</sup> Fixed-Bed Bioreactor. *Hum. Gene Ther. Methods* **2016**, *27*, 112–121.

(26) Piras, B. A.; Drury, J. E.; Morton, C. L.; Spence, Y.; Lockey, T. D.; Nathwani, A. C.; Davidoff, A. M.; Meagher, M. M. Distribution of AAV8 Particles in Cell Lysates and Culture Media Changes with Time and Is Dependent on the Recombinant Vector. *Mol. Ther. - Methods Clin. Dev.* **2016**, *3*, 16015.

(27) Wright, J. Product-Related Impurities in Clinical-Grade Recombinant AAV Vectors: Characterization and Risk Assessment. *Biomedicines* **2014**, *2*, 80–97.

(28) Dong, J.-Y.; Fan, P.-D.; Frizzell, R. A. Quantitative Analysis of the Packaging Capacity of Recombinant Adeno-Associated Virus. *Hum. Gene Ther.* **1996**, *7*, 2101–2112.

(29) Daya, S.; Berns, K. I. Gene Therapy Using Adeno-Associated Virus Vectors. *Clin. Microbiol. Rev.* **2008**, *21*, 583–593.

(30) Deverman, B. E.; Ravina, B. M.; Bankiewicz, K. S.; Paul, S. M.; Sah, D. W. Y. Gene Therapy for Neurological Disorders: Progress and Prospects. *Nat. Rev. Drug Discovery* **2018**, *17*, 641–659.

(31) Bucher, K.; Rodríguez-Bocanegra, E.; Daultbekov, D.; Fischer, M. D. Immune Responses to Retinal Gene Therapy Using Adeno-Associated Viral Vectors – Implications for Treatment Success and Safety. *Prog. Retin. Eye Res.* **2021**, *83*, 100915.

(32) Shirley, J. L.; de Jong, Y. P.; Herzog, C.; Herzog, R. W. Immune Responses to Viral Gene Therapy Vectors. *Mol. Ther.* **2020**, *28*, 709–722.